MIT Libraries | DSpace@MIT

MIT Open Access Articles

High active carrier concentration in n-type, thin film Ge using delta-doping

Massachusetts Institute of Technology

High active carrier concentration in n-type, thin film Ge using delta-doping

Rodolfo E. Camacho-Aguilera,[*] Yan Cai, Jonathan T. Bessette, Lionel C. Kimerling, and Jurgen Michel

MIT, Department of Materials Science & Engineering, 77 Massachusetts Avenue, Cambridge, MA 02139, USA
*rcamacho@mit.edu

Abstract: We demonstrate CVD in situ doping of Ge by utilizing phosphorus delta-doping for the creation of a high dopant diffusion source. Multiple monolayer delta doping creates source phosphorous concentrations above $1 \times 10^{20} \text{cm}^{-3}$, and uniform activated dopant concentrations above $4 \times 10^{19} \text{cm}^{-3}$ in a 600-800nm thick Ge layer after in-diffusion. By controlling dopant out-diffusion, near-complete incorporation of phosphorus diffusion source is shown.

©2012 Optical Society of America

OCIS codes: (310.1860) Deposition and fabrication; (310.3840) Materials and process characterization; (140.3380) Laser materials; (160.3130) Integrated optics materials.

References and links

1. L. C. Kimerling, D. Ahn, A. B. Apsel, M. Beals, D. Carothers, Y.-K. Chen, T. Conway, D. M. Gill, M. Grove, C.-Y. Hong, M. Lipson, J. Liu, J. Michel, D. Pan, S. S. Patel, A. T. Pomerene, M. Rasras, D. K. Sparacin, K.-Y. Tu, A. E. White, and C. W. Wong, "Electronic-photonic integrated circuits on the CMOS platform," Proc. SPIE **6125**, 612502 (2006).
2. R. Soref, "Silicon photonics: a review of recent literature," Silicon **2**(1), 1–6 (2010).
3. J. Michel, J. Liu, and L. C. Kimerling, "High-performance Ge-on-Si photodetectors," Nat. Photonics **4**(8), 527–534 (2010).
4. X. Sun, J. Liu, L. C. Kimerling, and J. Michel, "Room-temperature direct bandgap electroluminesence from Ge-on-Si light-emitting diodes," Opt. Lett. **34**(8), 1198–1200 (2009).
5. E. Kasper, M. Oehme, T. Aguirov, J. Werner, M. Kittler, and J. Schulze, "Room temperature direct band gap emission from Ge p-i-n heterojunction photodiodes," in *Proceedings of Group IV Photonics 2010* (2010).
6. P. Velha, K. Gallacher, D. C. Dumas, M. Myronov, D. R. Leadley, and D. J. Paul, "Direct band-gap electroluminescence from strained n-doped germanium diode," in *CLEO: Science and Innovations*, OSA Technical Digest (online) (Optical Society of America, 2012), paper CW1L.7.
7. S.-L. Cheng, J. Lu, G. Shambat, H.-Y. Yu, K. Saraswat, J. Vuckovic, and Y. Nishi, "Room temperature 1.6 μm electroluminescence from Ge light emitting diode on Si substrate," Opt. Express **17**(12), 10019–10024 (2009).
8. M. de Kersauson, R. Jakomin, M. El Kurdi, G. Beaudoin, N. Zerounian, F. Aniel, S. Sauvage, I. Sagnes, and P. Boucaud, "Direct and indirect band gap room temperature electroluminescence of Ge diodes," J. Appl. Phys. **108**(2), 023105 (2010).
9. J. Liu, X. Sun, R. Camacho-Aguilera, L. C. Kimerling, and J. Michel, "Ge-on-Si laser operating at room temperature," Opt. Lett. **35**(5), 679–681 (2010).
10. R. E. Camacho-Aguilera, Y. Cai, N. Patel, J. T. Bessette, M. Romagnoli, L. C. Kimerling, and J. Michel, "An electrically pumped germanium laser," Opt. Express **20**(10), 11316–11320 (2012).
11. X. Sun, J. Liu, L. C. Kimerling, J. Michel, and T. L. Koch, "Band-engineered Ge as gain medium for Si-based laser," in *Integrated Photonics and Nanophotonics Research and Applications (IPNRA) Topical Meeting,* (Boston, MA, USA, 2008).
12. X. Sun, J. Liu, L. C. Kimerling, and J. Michel, "Direct gap photoluminescence of n-type tensile-strained Ge-on-Si," Appl. Phys. Lett. **95**(1), 011911 (2009).
13. X. Sun, "Ge-on-Si light-emitting materials and devices for silicon photonics," Ph.D. dissertation (MIT, 2009).
14. S. Brotzmann and H. Bracht, "Intrinsic and extrinsic diffusion of phosphorus, arsenic, and antimony in germanium," J. Appl. Phys. **103**(3), 033508 (2008).
15. X. Sun, J. Liu, L. C. Kimerling, and J. Michel, "Optical bleaching of thin film Ge on Si," ECS Trans. **16**, 881–889 (2008).
16. A. Satta, E. Simoen, R. Duffy, T. Janssens, T. Clarysse, A. Benedetti, M. Meuris, and W. Vandervorst, "Diffusion, activation, and regrowth behavior of high dose P implants in Ge," Appl. Phys. Lett. **88**(16), 162118 (2006).

17. S. J. Bass, "Silicon and germanium doping of epitaxial gallium arsenide grown by the trimethylgallium-arsine method," J. Cryst. Growth **47**(5-6), 613–618 (1979).
18. C. E. C. Wood, G. Metze, J. Berry, and L. F. Eastman, "Complex free-carrier profile synthesis by 'atomic-plane' doping of MBE GaAs," J. Appl. Phys. **51**(1), 383–387 (1980).
19. H. Gossmann, A. M. Vredenberg, C. S. Rafferty, H. S. Luftman, F. C. Unterwald, D. C. Jacobson, T. Boone, and J. M. Poate, "Diffusion of dopants in B- and Sb-delta-doped Si films grown by solid-phase epitaxy," J. Appl. Phys. **74**(5), 3150–3155 (1993).
20. G. Scappucci, G. Capellini, W. C. T. Lee, and M. Y. Simmons, "Ultradense phosphorus in germanium delta-doped layers," Appl. Phys. Lett. **94**(16), 162106 (2009).
21. G. Scappucci, G. Capellini, W. M. Klesse, and M. Y. Simmons, "Dual-temperature encapsulation of phosphorus in germanium delta layers toward ultra-shallow junctions," J. Cryst. Growth **316**(1), 81–84 (2011).
22. Y. Cai, R. Camacho-Aguilera, J. T. Bessette, L. C. Kimerling, and J. Michel, "High phosphorus doped germanium: dopant diffusion and modeling," J. Appl. Phys. **112**(3), 034509 (2012).
23. H.-C. Luan, D. R. Lim, K. K. Lee, K. M. Chen, J. G. Sandland, K. Wada, and L. C. Kimerling, "High-quality Ge epilayers on Si with low threading-dislocation densities," Appl. Phys. Lett. **75**(19), 2909–2911 (1999).
24. S.-M. Jang, K. Liao, and R. Reif, "Chemical vapor deposition of epitaxial silicon-germanium from silane and germane. II. In situ boron, arsenic, and phosphorus doping," J. Electrochem. Soc. **142**(10), 3520–3527 (1995).
25. R. Camacho-Aguilera, Z. Han, Y. Cai, J. Bessette, L. Kimerling, and J. Michel, "Band gap narrowing in highly doped Ge," submitted (2012).
26. R. Olesinski, N. Kanani, and G. Abbaschian, "The Ge−P (germanium-phosphorus) system," J. Phase Equilibria **6**, 262–266 (1985).

1. Introduction

Germanium has emerged as a candidate for fully CMOS integrated light emitters to enable photonics circuits [1–3]. Recently Ge based LEDs [4–8] and laser [9,10] have been demonstrated, emitting in the near-infrared (NIR). A Ge based, CMOS integrated light source opens the potential for fully scalable photonic integration. In order to achieve this goal, the requirements for efficient Ge light emitting devices are listed below.

A combination of strain and doping in Ge can open a very efficient recombination path through the direct Γ-valley [11] enabling inversion and gain. The gain is directly dependent of the n-type doping level and increases superlinearly with n-type doping [12]. Furthermore, crystalline quality of the Ge affects absorption and recombination paths for carriers and photons in a light emitter. When using ultra high vacuum chemical vapor deposition (UHV-CVD) to grow Ge epi-layers, n-type doping during growth is concentration limited [13] in order to maintain low defect densities. The maximum theoretically expected active dopant concentration for UHV-CVD n-type Ge is $2 \times 10^{19} \text{cm}^{-3}$ [14] and experimentally a phosphorus (P) doping concentration of $1.2 \times 10^{19} \text{cm}^{-3}$ was demonstrated [15]. CVD in situ doping concentrations are limited by a delicate balance between P out-diffusion and Ge growth temperature for high quality films.

Higher doping concentrations for in situ doped Ge films are possible when using non-equilibrium growth methods like molecular beam epitaxy (MBE). For MBE growth a n-type doping concentration of $1 \times 10^{20} \text{cm}^{-3}$ has been demonstrated [5]. However, it is very challenging to integrate MBE grown Ge films into a CMOS process flow due to high capital cost and low throughput. Ion implantation, another commonly used method to introduce dopants into Ge, causes significant lattice damage such that, after the implantation, samples have to be annealed at temperatures above 600°C. The lattice damage increases vacancies and other defect concentrations that act as recombination centers and cause increased optical absorption as well as donor compensation, decreasing the active dopant concentration. High diffusivity of the dopants prohibits anneals at higher temperatures to remove the implantation related defects. In order to slow down the dopant loss, diffusion barriers of silicon oxide or silicon nitride have been used [14,16]. The doping method presented in this paper provides high n-type dopant concentrations, good crystallinity, and requires low annealing temperatures to prevent out-diffusion.

Delta doping has been used in compound semiconductors [17,18], Si [19], and MBE grown Ge [20,21] to significantly increase doping levels locally. Scappucci et al. [20,21] showed that delta doping was possible through low temperature deposition of Ge. Here we

present a similar process to increase the P-doping concentration in Ge to above $4 \times 10^{19} \text{cm}^{-3}$, while retaining single crystallinity and utilizing a CMOS process. In order to reach high doping levels we utilize dopant enhanced diffusion of P in already P-doped Ge films. The enhanced diffusivity is necessary to limit P out-diffusion while increasing the P concentration in the active device area. A detailed description of the diffusion mechanism can be found elsewhere [22]. In this paper we will describe the epitaxial growth process that yields P concentrations in Ge in the mid 10^{19}cm^{-3}.

2. Thin film Ge growth

Ge films were grown epitaxially on bulk silicon substrates with (100) orientation by UHV-CVD. Here we use the same growth process as has been described previously [15,23]. The films were deposited in a two-step process beginning with a low-temperature deposition of a thin, but highly defective Ge buffer epitaxy layer. On top of the buffer layer, a high-temperature (650°C) growth of P doped Ge creates a thick layer of high quality crystalline n^+ Ge with an activated P concentration of up to 1.2×10^{19} cm^{-3} [22]. To retain the high quality n^+Ge layer, a higher concentration P diffusion source is deposited on top of this active device layer. Since higher than $1.2 \times 10^{19} \text{cm}^{-3}$ doping levels of P cannot be achieved with in situ doping of Ge using UHV-CVD, a new growth process was developed that would increase the activated P doping level without introducing additional defects in the active device layer. The dopant source can be created by introducing mono-layers of P on Ge (delta layers). P adheres to Ge at low temperatures without growing epitaxially. Due to the accommodation coefficient of Ge-P, only mono-atomic P delta layers are allowed on the Ge surface.

The dopant source concentration depends on the amount of deposited layers. A single monolayer surface concentration of $\sim 5 \times 10^{14} \text{cm}^{-2}$ is equivalent to $\sim 1 \times 10^{19} \text{cm}^{-3}$ P if fully incorporated into a 500nm layer. The process demonstrated here shows a multilayer structure with an expected concentration of $\sim 4 \times 10^{19} \text{cm}^{-3}$. During deposition of the monolayers, or delta layers, surfactant poisoning effect is observed on the Ge surface stemming from P, decreasing the growth rate of any subsequent Ge layer [24]. This effect has been observed before in Si and Si:Ge alloys [13]. Ge atoms cannot interchange the positions taken by P on the Ge surface, leading to growth stop. A schematic of the complete growth process is illustrated in Fig. 1 where the dopant reservoir depicts several P delta layers.

Intrinsic undoped Ge growth rate is higher than P-doped Ge growth rate and its slower P diffusion rate in Ge retains the P delta layers. Hence, the P delta layers are encapsulated by intrinsic undoped Ge to form a P diffusion source for the active device layer. The delta doped source layer exhibits a higher P diffusivity compared to undoped Ge due to dopant enhanced diffusion [22] caused by the high P concentration. The delta doped Ge-P layers act as dopant source, not affecting the crystallinity or defect concentration of the active device layer of high temperature growth crystalline Ge.

The multilayer structure is fabricated from a series of 4 alternating layers of undoped Ge and P deposited at 400°C and 450°C, respectively, so as to obtain P concentrations close to $5 \times 10^{19} \text{cm}^{-3}$.
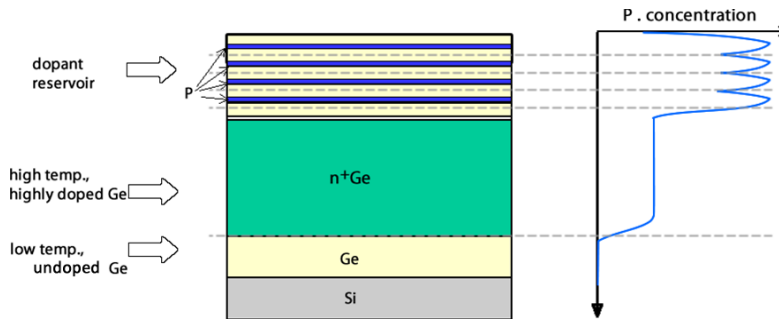
Fig. 1. Schematic of the growth layers. The dopant reservoir are alternating layers of Ge and P. Dopant concentration in Ge increases dramatically in the dopant reservoir without being linear due to slow diffusion into the intrinsic undoped Ge used in the layers.

Although the P concentration in the Ge film is significantly increased using this modified growth process, Hall Effect measurements on as-grown samples, presented in the following section, suggest that the P dopants are not fully activated. Similarly, photoluminescence (PL) measurements show that the direct bandgap Ge light emission from these samples, absent further processing, is less efficient than that from reference samples without P delta doping. Therefore, low PL from delta doped samples indicates that thermal treatment after deposition can activate the dopants.

The samples were thermally annealed under Nitrogen flow by rapid thermal annealing (RTA) using an AG Associates Heatpulse 410. The temperature ranged from 550 to 800°C with annealing times in the range of 30 to 300 seconds. In order to prevent dopant out-diffusion and oxidation, a thin 100nm SiO_2 was deposited by plasma enhanced chemical vapor deposition (PE-CVD) using an Applied Materials Centura 5300 DCVD system.

Surface morphology changes with growth process and annealing times were observed. Figures 2(a) and 2(b) show Ge films grown using a standard in situ P doped epi growth [23] and a delta doped growth. The doping concentration of the delta doped films varies, ranging from 2 to 4.5 $\times$ 10^{19}cm^{-3}. Comparing these results with standard epi-growth shows a significant increase in roughness after delta doping due to the arrest in epitaxial growth in the delta doped growth. Nevertheless, the roughness does not change the active carrier concentration but only increases the light scattering at the surface, as can be seen in PL intensity measurements.
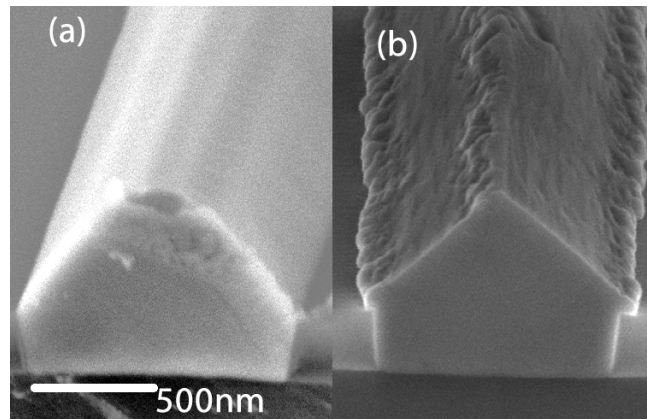

Fig. 2. SEM images of (a) in situ doped Ge and (b) delta doped Ge grown with source grown at 400C. Notice difference in surface roughness which indicates the arrest of epitaxial growth.

Surface roughness of 35-50nm root-mean-square (RMS) is measured in all samples after delta-doping. In comparison, an atomically flat Ge surface has a roughness of ~5nm RMS. Annealing conditions above 600°C will decrease the surface roughness. However, in order to obtain atomically flat surfaces the required temperatures are close to the melting point of Ge. Such high temperatures would have an adverse effect in the dopant concentration.

3. Experimental results

In order to evaluate if the active P doping can be increased in the high quality Ge film secondary ion mass spectrometry (SIMS) was used to determine the total P concentration in the Ge films and Hall Effect measurements were used to determine the activated P concentration. SIMS profiles for delta doping at 400°C and 450°C are shown in Fig. 3. As can be seen in Fig. 3, the total P concentration in the delta doped region is above the predicted maximum P concentration [14] and is significantly higher than in situ doped, UHVCVD grown Ge. The figure also shows that P diffusion already occurs at the growth temperature. At 450°C, P has diffused from the delta layer further into the in situ doped Ge region than at 400°C, obtaining a uniform P concentration dopant source. The SIMS profiles furthermore highlight the dopant accumulation at the Ge-Si interface at the bottom of the Ge layer. Due to the growth process, the initial 60nm thick Ge buffer layer is highly dislocated, providing a sink for fast diffusing dopant atoms. The average active carrier concentrations for the 400°C and 450°C growths were determined by Hall Effect measurements to be $1.5 \times 10^{19} \mathrm{cm}^{-3}$ and $1.8 \times 10^{19} \mathrm{cm}^{-3}$, respectively. The discrepancy between active carrier concentration and total dopant concentration clearly shows that defects limit the dopant activation.
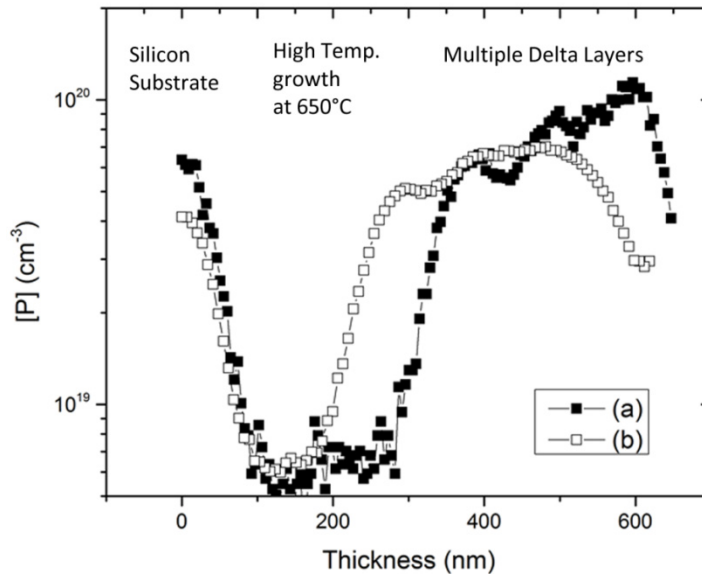

Fig. 3. SIMS profiles of as-grown P delta doped Ge, with P deltas grown at (a) 400°C and (b) 450°C. Dopant diffusion from delta source increases the concentration of P in the underlying high temperature Ge region.

An example for the P redistribution due to annealing is shown in Fig. 4 SIMS results. A 400°C delta doped Ge films were annealed at 600°C for 30 and 60 seconds, and 700°C for 30 seconds. A fairly even distribution of P in the in situ doped Ge region due to P out-diffusion from the delta doped range can be observed. The average P concentration in the in situ doped region is about $4 \times 10^{19} \mathrm{cm}^{-3}$ after 30sec at 700°C annealing. Annealing improves the P

concentration by at least a factor of 3 as seen in Fig. 4. Since P is diffused into Ge of high crystalline quality, it is expected that the in-diffused P is completely activated.
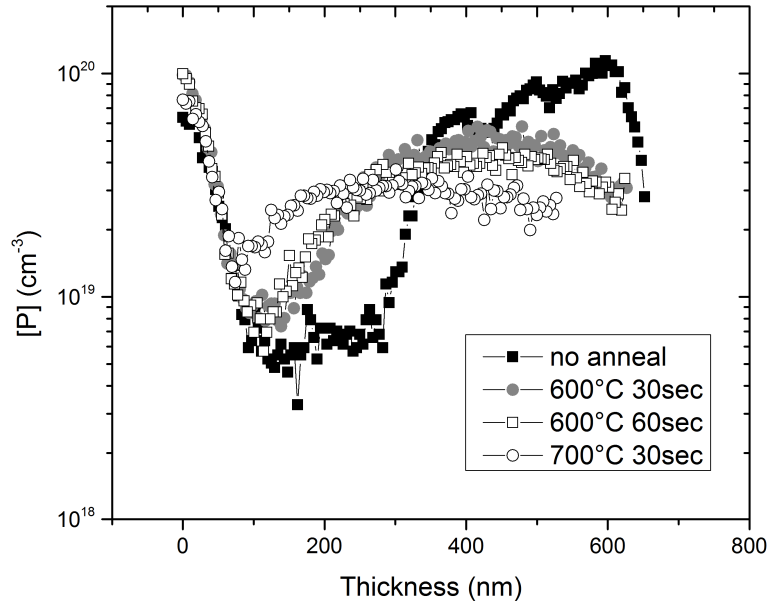

Fig. 4. SIMS profiles of dopant redistribution from delta doped Ge grown at 400°C. The diffusion of the dopant is time and temperature dependent, becoming more uniform at higher temperatures but limited by outdiffusion at longer times.

It is observed that the active carrier concentration increases with annealing, however, the active carrier concentration typically increases up to a certain annealing temperature and then decreases. Agglomeration of dopants on the Si interface due to misfit dislocations and the lower dopant concentration on the Ge surface after extended anneals prove that out-diffusion is the mechanism for dopant lose. This leads to each temperature having an optimal time for maximizing active carrier concentration, preventing out-diffusion loses. The PL intensity increases as the active carrier concentration achieves the maximum capable per annealing temperature and time. Since Hall Effect measures the integrated carrier concentration of the delta doped region as well as the in situ doped region, it is very difficult to determine the optimal annealing conditions from these data.

It was therefore important to find an additional indicator of the quality and active doping level of the Ge films. It was found that band gap narrowing in Ge correlates to the active n-type doping. As the active doping level increases the direct band gap of Ge narrows, which is observable in PL measurements. More details can be found in Camacho-Aguilera et al. [25]. An example of the highest PL intensities and the accompanying shifts is shown in Table 1. The emission intensities are not normalized for Ge thickness. It is obvious that the samples with the largest red-shift show the highest PL intensity. PL intensity depends heavily on dopant concentration and crystal quality [24]. At low annealing temperatures, the dopant concentration is high while the PL intensity is low. One possible explanation of this effect is that annealing at high temperatures reduces defects, resulting in lower loses from the Ge crystal matrix.

Table 1. Photoluminescence at RT of Delta Doped Ge Samples under Different RTA Conditions

Anneal (°C)	no anneal	600		700		standard epi-Ge
Time (sec)	-	30	60	30	60	-
Peak emission (nm)	1640	1659	1662	1642	1650	1603
Hall effect active carrier concentration ($\times 10^{19} cm^{-3}$)	1.9	3.8	4.3	4.2	3.4	1.1
PL integrated Intensity (a.u. $\times 10^{-2}$)	0.742	2.04	1.73	1.5	1.3	1.18

As seen in Table 1, PL decreases with increasing annealing time even though the active carrier concentration increases, suggesting that doping decreases with increasing annealing times. Out-diffusion is the mechanism governing the PL intensity loss at longer annealing times. However, the active carrier concentration does not increase past a certain value that is given by the solid solubility. Olesinski et al. [26] determined that the solid solubility of P in Ge at 775°C is $8 \times 10^{19} cm^{-3}$. Figure 5 shows the maximum active carrier concentration that was found for different temperatures and annealing times and compares the concentrations to the solid solubility of P in Ge. As can be seen from Fig. 5, P reaches near solid solubility at temperatures below 550°C. Above 550°C, the maximum active carrier concentration is always smaller that the solid solubility of P, decreasing above 600°C despite the increase of the solid solubility. The disparity is caused by the competition of P dopant loss due to out-diffusion and defect annealed, which permits active dopants. P incorporation is also limited by the diffusion source, which contained $\sim 4 \times 10^{19} cm^{-3}$. Maximum dopant activation was almost reached for the quantity available in the delta doped source. Hence, short annealing times at higher temperatures, coupled with an effective diffusion barrier and a higher doped diffusion source, are expected to yield better P incorporation overcoming dopant loss.
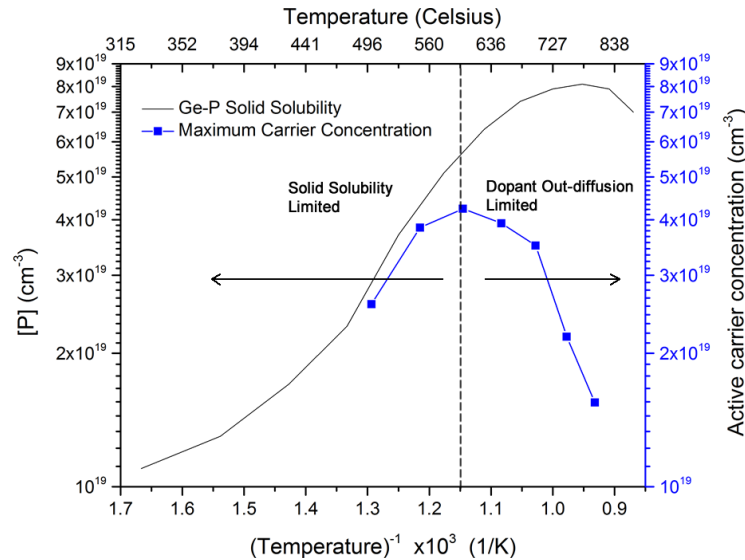

Fig. 5. Comparison of P solid solubility [26] in Ge and observed maximum active carrier concentration of delta doping at different temperatures.

The increase in dopant concentration is made possible by a dopant source with concentrations of $>2 \times 10^{20} \text{cm}^{-3}$ and enhanced dopant diffusion [22]. The diffusion source can be removed from the active device layer through chemical mechanical polishing (CMP) for use in active light emitting devices [10].

4. Conclusion

We have demonstrated a method to create high active P concentrations in high quality crystalline Ge films using epitaxial CVD growth. Fully incorporated multi-layered delta doping provides a high chemical activity source for achieving active carrier concentrations above $4 \times 10^{19} \text{cm}^{-3}$. The main mechanism limiting the maximum carrier concentration is the out-diffusion of the dopants. The multi-layered dopant diffusion source is a critical element of the diffusion design to solve the main issues in high dopant concentrations in Ge. Selective growth of the delta doped Ge grown films makes them a suitable candidate for CMOS compatible Ge diode lasers.